



Longitudinal Deformation of the Right Ventricle in Hypoplastic Left Heart Syndrome: A Comparative Study of 2D-Feature Tracking Magnetic Resonance Imaging and 2D-Speckle Tracking Echocardiography

Mona Salehi Ravesh¹ · Carsten Rickers¹ · Finn Jonathan Bannert¹ · David Hautemann² · Abdullah Al Bulushi^{1,3} · Dominik Daniel Gabbert¹ · Philip Wegner¹ · Eva Kis^{1,4} · Jan Hinnerk Hansen¹ · Michael Jeresch-Herold⁵ · H.-H. Kramer¹ · Jana Logoteta¹

Received: 6 December 2017 / Accepted: 2 May 2018 / Published online: 10 May 2018
© Springer Science+Business Media, LLC, part of Springer Nature 2018

Abstract

In hypoplastic left heart syndrome (HLHS), long-term outcome is closely related to right ventricular function. Echocardiography and magnetic resonance imaging (MRI) are routinely used for functional assessment. MRI 2D-tissue feature tracking (2D-FT) allows quantification of myocardial deformation but has not yet been applied to HLHS patients. We sought to investigate the feasibility of this technique and to compare the results to 2D-speckle tracking echocardiography (2D-STE). In routine MRI 2D anatomical four chamber view, cine images were recorded in 55 HLHS patients (median age 4.9 years [1.6, 17.0]). Regional and global peak systolic longitudinal strain (LS) and strain rate (LSR) were determined using 2D-FT software. Echocardiographic four chamber view was analyzed with 2D-STE. Visualization of all myocardial segments with MRI was excellent, regional, and global LS and LSR could be assessed in all data sets. In 2D-STE, 28% of apical segments could not be analyzed due to poor image quality. Agreement of 2D-FT MRI and 2D-STE was acceptable for global LS, but poor for global LSR. In MRI, regional LS was lower in the septal segments, while LSR was not different between the segments. GLS and GLSR correlated with ejection fraction (GLS: $r = -0.45$ and $r < 0.001$, GLSR: $r = -0.34$ and $p = 0.01$). With new post-processing options, the assessment of regional and global LS and LSR is feasible in routine MRI of HLHS patients. For LS, results were comparable with 2D-STE. The agreement was poor for LSR, which might relate to differences in temporal resolution between the two imaging modalities.

Keywords Hypoplastic left heart syndrome · Right ventricular function · Magnetic resonance imaging (MRI) · Feature tracking MRI · Strain and strain rate · Dyssynchrony

✉ Mona Salehi Ravesh
Mona.Salehiravesh@uksh.de

- ¹ Department of Congenital Heart Disease and Pediatric Cardiology, University Hospital Schleswig-Holstein (UKSH), Campus Kiel, Arnold-Heller-Street 3, Building 9, 24105 Kiel, Germany
- ² Medis Medical Imaging Systems BV, Leiden, The Netherlands
- ³ Department of Pediatric Cardiology, National Heart Centre, Royal Hospital, Muscat, Oman
- ⁴ Hungarian Institute of Cardiology, Pediatric Heart Centre, Budapest, Hungary
- ⁵ Department of Radiology, Brigham & Women's Hospital, Boston, MA, USA

Introduction

In HLHS, the right ventricle (RV) operates as the single pumping chamber and has to support the systemic circulation. Impaired RV function is associated with morbidity and mortality throughout all stages of Fontan palliation and during follow up [1–3]. Therefore, quantitative assessment of RV function in HLHS patients is essential between operative stages and during follow up. Echocardiography and nowadays cardiac magnetic resonance (CMR) imaging are routinely used for imaging of the single RV. In recent years, 2D-STE has been successfully used for measuring regional and global myocardial deformation parameters in HLHS patients [4–7]. 2D-STE global longitudinal strain rate

has been shown to correlate with ventricular elastance, a parameter of contractility [5]. But there are a number of intrinsic limitations to the 2D-STE technique, the most critical being the temporal instability of tracking patterns [8]. Due to through-plane motion, physiological changes of living tissue structures and changes of interrogation angles between moving tissue and ultrasonic beam speckle patterns are not stable temporally. Recently, 2D-tissue feature tracking is used to analyze myocardial deformation parameters in MRI [9]. This technique has already been applied to Fontan patients with heterogeneous univentricular hearts [10, 11] including single left and right ventricles. The purpose of this study was to investigate the feasibility of 2D-FT MRI in a uniform cohort of HLHS patients and to compare the results with 2D-STE.

Materials and Methods

Patients

The study population consists of 55 HLHS patients. In all patients, a modified Norwood procedure with modified Blalock-Taussig shunt was performed as stage one, followed by a superior cavo-pulmonary anastomosis (Hemi-Fontan, BCPC) as stage two. In 41 patients, a fenestrated intra-atrial lateral tunnel modification of the total cavopulmonary anastomosis (TCPC) procedure was performed as stage three of the palliative operations.

All children underwent echocardiography and MRI as part of a routine clinical examination. In order to compare 2D-STE and 2D-FT MRI, only datasets of patients that underwent echocardiography and CMR examination within three months were used for analysis. A total of 46 datasets fulfilled this criterion.

Demographic Data

Pertinent patient data were collected and included age at examination, gender, weight, body surface area (BSA), New York Heart Association (NYHA) functional class, medication, patency of the fenestration, grade of tricuspid valve regurgitation, transcutaneous oxygen saturation (SO₂) level, and number of surgical procedures (Table 1).

Cardiac MRI

All CMR examinations were performed on a 3.0 T MR system (Achieva TX-series; Philips Healthcare, Best, The Netherlands) using a 32 channels XL SENSE Torso/Cardiac surface coil (Philips Healthcare, Best, The Netherlands). If necessary, patients under 10 years were sedated with midazolam and propofol according to institutional protocol

Table 1 Patients demographics, clinical characteristics and CMR data

	N=55
Patient demographics	
Hemi-Fontan	14
Fontan	41
Male gender, n (%)	41 (75)
Age at exam, (years)	4.9 [1.6, 17.0]
Weight (kg)	19.0 [9.6, 72.0]
BSA (m ²)	0.74 [0.48, 1.84]
Clinical characteristics	
Number of operations (2/3/4/5/6/7)	4/27/16/4/3/1
Open fenestration, n (%)	33 (60)
NYHA class (I/II/III/IV)	31/21/2/0
Medication (ACE/D/BB)	6/4/2
Oxygen saturation (%)	90 [73, 98]
CMR data	
Heart rate (bpm)	81 [51, 112]
EF (%)	55 [31, 69]
TR (mild/moderate/severe)	50/5/0

All non-normal distributed continuous variables are given as median, minimum, and maximum values

ACE angiotension converting enzyme inhibitors, BB beta-blockers, BSA body surface area, D diuretics, EF ejection fraction, TR tricuspid regurgitation

without ventilation. Heart rate (HR), blood pressure, and SO₂ level were monitored during the examinations.

High resolution four chamber view data sets were acquired with a T₁-weighted/balanced 2D-cine MR pulse sequence using SENSE techniques [12], with the following imaging parameters: repetition time/echo time: 3.3/1.6 ms; flip angle: 40°; mean field of view: from 238×205 (child) to 334×300 (adult) mm², image matrix: 244×244 to 299×299 pixels; 1 slice, SENSE factor: 1.5; median heart phases: 25 [20, 30], number of signal averages: 2; slice thickness: 5 (child)/7 (adult) without interslice gap, median temporal resolution: 28.8 [21.5, 54] ms, and total acquisition time of less than 30 s.

End-diastolic, end-systolic, and stroke volume as well as ejection fraction (EF) were determined using QMass (version 7.6, Medis medical imaging systems bv, Leiden, The Netherlands). Volumes were indexed to BSA.

For 2D-FT MRI, the module QStrain in Medis Suite MR (version 2.1, Medis Medical Imaging Systems BV, Leiden, The Netherlands) was used [13]. After manually setting the cine frame with smallest RV cavity area as end-systolic, the frame with largest as end-diastolic heart phase and tracing of the endo- and epicardial border in both phases, the RV was automatically divided into seven segments (Fig. 1). For each segment, peak longitudinal strain (LS, percent change in segment length from end diastole) and peak longitudinal strain rate (LSR, representing rate of myocardial deformation)

Fig. 1 Myocardial segmentation using 2D-FT MRI (left) and 2D-STE (right) of a HLHS patient with mitral and aortic atresia. In order to compare the two techniques, the segmentation was adapted and only three segments (septal, apical, and lateral) remained

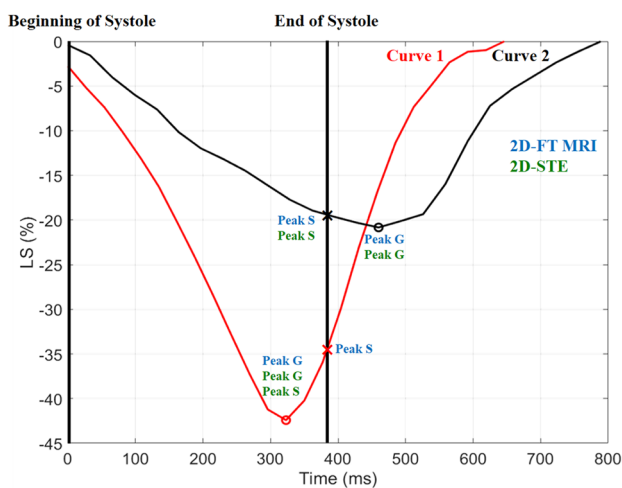
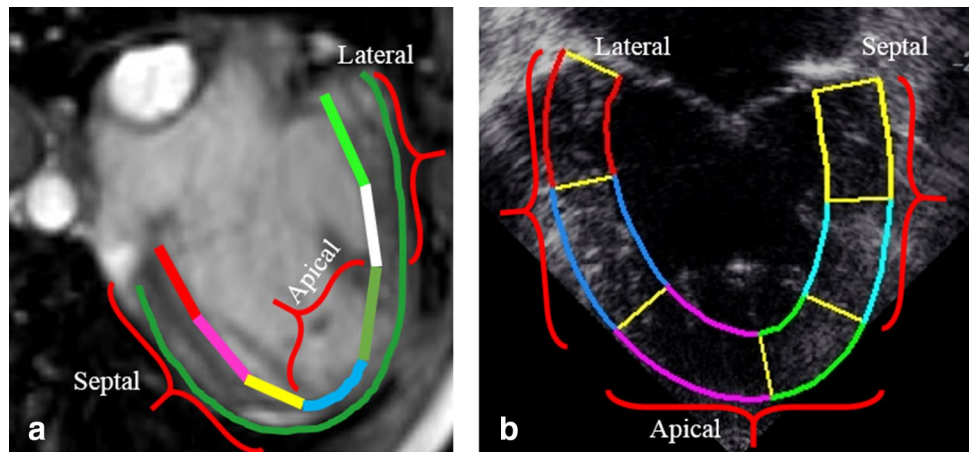


Fig. 2 Definition of peak strain in the 2D-FT MRI and 2D-STE. During a heart cycle, peak strain can occur during a systolic (curve 1) or a post systolic (curve 2) heart phase. The peak global strain (peak G) in both imaging modalities is defined as peak strain during one heart cycle independent of heart phase. However, peak systolic strain (peak S) is defined differently in MRI and STE. In 2D-FT MRI, peak S is defined as strain at the end of systole, while in 2D-STE, it is defined as peak strain during systole. Therefore, peak S in curve 2 with postsystolic shortening is equal in both imaging modalities, while in curve 1 with peak shortening during systole peak S is different between MRI and echocardiography

were recorded (Fig. 2). The measurements were repeated twice and averaged. Global LS (GLS) and LSR (GLSR) value were calculated as the mean of all segments.

Echocardiography

All echocardiographic recordings were obtained using a GE Vivid 7 system (General Electric Healthcare, Wauwatosa, Wisconsin, USA) and stored digitally for offline analysis. Gray scale images optimized for 2D-STE analysis were acquired from the apical four chamber view. Images were

obtained at a median frame rate of 85 in a range of 37–94 frames per second. One experienced echocardiographer (J. L.) analyzed the data offline using dedicated software (EchoPac, version 113, General Electric Healthcare, Wauwatosa, Wisconsin, USA). After manual tracing of the endocardial borders, the software divided the RV automatically into six segments. Segments were excluded, if the myocardium was not visualized well enough to allow speckle tracking. The peak LS and peak LSR were recorded for each segment. From the segmental data, GLS and GLSR were calculated as average of all available segments.

Comparison of 2D-FT MRI and 2D-STE

Both 2D-FT MRI and 2D-STE allow the measuring of endocardial, myocardial, and epicardial LS and LSR. In this study, we only calculated myocardial LS and LSR, since the endocardial and epicardial parameters are more affected by spatial resolution which differs substantially between the MR and echocardiographic images. In order to compare the two techniques, the segmentation had to be adapted, since the 2D-FT MRI uses seven segments while 2D-STE divides the chamber into six segments. We, therefore, joint the segments in such a way that for both imaging modalities only three segments (septal, apical, and lateral) remained. These are defined as follows in 2D-FT MRI: (septal = basal inferoseptal + mid inferoseptal + apical septal; apical = apex + apical lateral; lateral = mid anterolateral + basal anterolateral) and in 2D-STE: (septal = basal septal + mid septal; apical: apical septal + apical lateral, lateral = mid lateral + basal lateral) and shown in Fig. 1.

To be able to compare peak strain of 2D-FT MRI and 2D-STE, peak global strain (Peak G) not peak systolic strain (Peak S) was measured. The Peak G in both imaging modalities is defined as peak strain during one heart cycle independent of heart phase. However, the Peak S is defined differently in 2D-FT MRI and 2D-STE. In 2D-FT MRI, Peak S is defined

as strain at the end of systole, while in 2D-STE, it is defined as peak strain during systole (Fig. 2).

Intraventricular Dyssynchrony

In 2D-FT MRI, the time interval from the end of diastolic heart phase to the peak of myocardial LS (time to peak LS, T2PLS) was obtained for each segment. In 2D-STE, the T2PLS was determined as the time interval from the beginning of the QRS interval to peak myocardial LS for each segment. The wall-to-wall delay was calculated by subtracting the time interval of the basal septal segment from that of the basal lateral segment.

Reproducibility

To assess interobserver variability, two blinded observers (M. S.R. and F.J. B.) analyzed all 55 data sets twice. The determination of the interobserver variability was based on the calculated mean values of the first and second analysis of each observer. M.S.R. analyzed all data sets twice at least 4 weeks apart to calculate intraobserver variability. Reproducibility of 2D-STE parameters in HLHS patients has previously been reported by our group and was not repeated in this study [7].

Statistical Analysis

All continuous variables are given as mean value with standard deviation or median and range of the lowest and highest values, depending on data distribution. *P* values for comparison of two groups were obtained from Student's *t* test or a Mann–Whitney *U* test as appropriate. Normality (Gaussian distribution) was tested for all continuous variables using the Shapiro–Wilk test. Comparisons between multiple groups were made with ANOVA or Kruskal–Wallis as appropriate. If the test was positive, post-hoc pairwise comparison of subgroups was performed (Scheffé's method for ANOVA and Conover for Kruskal–Wallis). Correlation coefficients were calculated using Pearson's or Spearman's formula depending on data distribution. Intra- and inter-observer variability were assessed using the coefficient of variation (CoV). A *p* value < 0.05 was considered statistically significant. For statistical analysis and preparation of graphs and Bland–Altman plots, the R Statistic package (Version 3.2.3, R Foundation for Statistical Computing, Vienna, Austria) and MedCalc (version 14.12.0, Ostend, Belgium) were used.

Results

Patient Characteristics

Pertinent patient data are given in Table 1. Most patients (96%) had no, or only a slight limitation of physical activity

(NYHA classes I and II). Ejection fraction in CMR was within the normal range for children in all patients and only five of the patients had moderate tricuspid regurgitation.

Regional and Global LS and LSR in BCPC and TCPC Using 2D-FT MRI

All 55 MRI data sets had a good image quality without any artifacts impairing segmental analysis. The assessment of regional and global LS and LSR could be performed in all data sets. In BCPC and TCPC, the regional values of all three segments were in the same range for LS (septal: *p* = 0.83, apical: *p* = 0.21, lateral: *p* = 0.74, global: *p* = 0.23) and LSR (septal: *p* = 0.25, apical: *p* = 0.28, lateral: *p* = 0.11). For GLS, there was no difference between two groups (*p* = 0.23). GLSR was significantly different between BCPC and TCPC (− 1.33 vs. − 1.18 s^{−1}, *p* = 0.04). Moreover, EF and NYHA class were not different between the groups: (BCPC vs. TCPC: EF: 55% [50, 66] vs. 52% [31, 69], *p* = 0.80; NYHA (I/II/III/IV): 3/11/0/0 vs. 28/10/2/0, *p* = 0.40). Since GLSR is the only parameter that is different between the groups, we regarded all patients as one group for the following analysis.

Regional and Global LS and LSR Using 2D-FT MRI and 2D-STE

Results of the regional and global LS and LSR of both imaging modalities are shown in Table 2 and Fig. 2. In 2D-FT MRI, the LS was lower in the septal segments, while LSR did not differ between the segments. In 2D-STE, the septal segments likewise showed the lowest LS and also LSR. 28% of apical segments could not be analyzed with 2D-STE due to poor image quality.

Comparison of Imaging Modalities

Bland–Altman plots show that there was acceptable agreement between GLS derived by 2D-FT MRI and 2D-STE (Fig. 3), while MRI slightly underestimates GLS. The agreement for the regional LS was not as good, being poor in

Table 2 Comparison between regional and global longitudinal strain and strain rate using 2D-FT MRI and 2D-STE

2D-FT MRI vs. 2D-STE	Regional			Global
	Septal	Apical	Lateral	
<i>p</i> value				
LS (%)	0.001	0.73	0.001	0.007
LSR (1/s)	0.001	0.12	0.01	0.13

Data are given in Fig. 4

LS longitudinal strain, LSR longitudinal strain rate

the apical segments. The agreement between the two methods for LSR was poor for global, as well as for the regional segments (Fig. 4).

Intraventricular Systolic Dyssynchrony

Table 3 shows the T2PLS in the septal and lateral segments for both imaging modalities. Time intervals measured by 2D STE are significantly longer than the T2PLS measured with 2D-FT MRI. This finding most likely relates to the different ways to identify the end of diastole in both methods.

Nevertheless, the basal septal to basal lateral wall-to-wall delay was not different, although the median of the differences was positive in 2D-FT MRI and negative in 2D-STE.

Correlation of GLS and GLSR with Demographic and Clinical Data

GLS, GLSR derived from MRI did not correlate with age, BSA, and SO_2 level. There is a significant negative correlation with EF for GLS and GLSR (GLS: $r = -0.45$ and $p < 0.001$, GLSR: $r = -0.34$ and $p = 0.01$). HR did

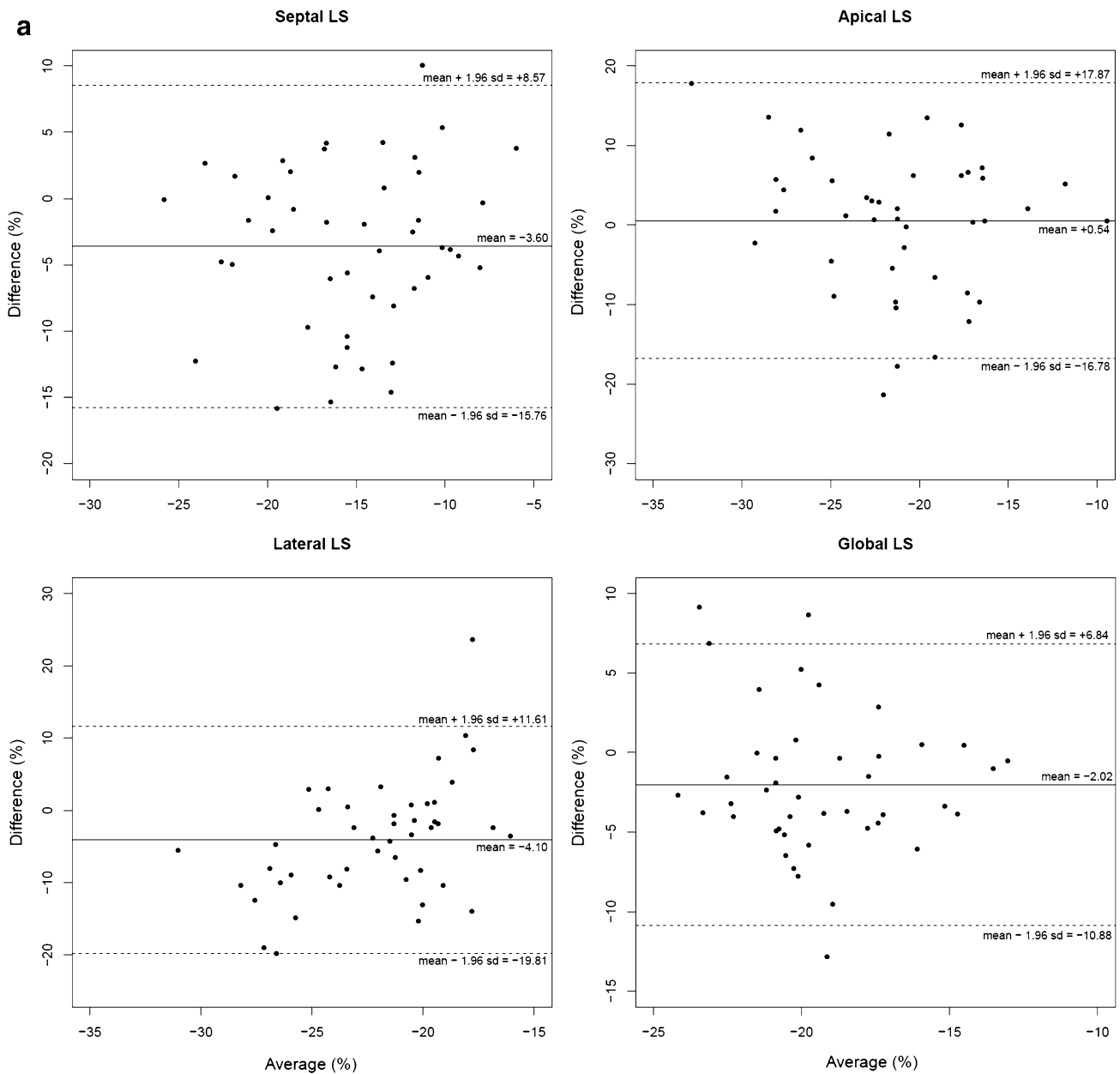


Fig. 3 Bland–Altman plots comparing 2D-FT MRI to 2D-STE. Horizontal solid lines represent the mean difference (2D-FT MRI—2D-STE) and the dashed lines mean \pm 1.96 standard deviation of the differences

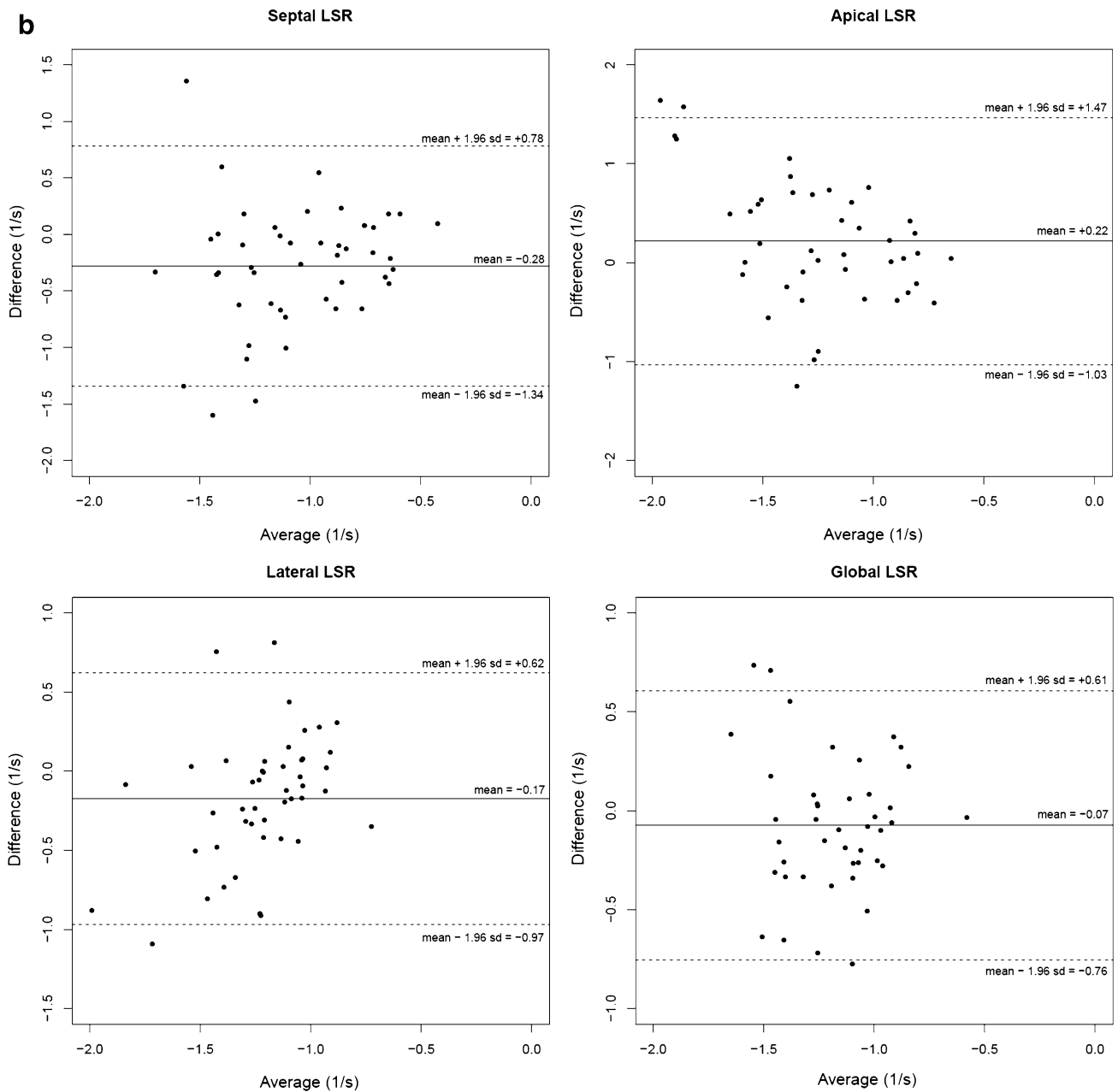


Fig. 3 (continued)

not correlate with GLS ($r = -0.03$ and $p = 0.85$), but with GLSR ($r = -0.43$ and $p = 0.001$). GLS and GLSR did not differ between NYHA I and II (GLS: -21.4% [$-25.6, -13.3$] vs. -19.6% [$-27.4, -14.0$], $p = 0.30$; GLSR: -1.23 [$-1.95, -0.60$] vs. -1.18 [$-2.21, -0.73$] s^{-1} , $p = 0.87$). The GLS and GLSR of male and female patients were in the same range (male vs. female: GLS: -19.8% [$-27.4, -13.3$] vs. -23.2% [$-25.5, -14.0$], $p = 0.22$; GLSR: -1.19 [$-2.21, -0.59$] vs. -1.23 [$-1.95, -0.72$] s^{-1} , $p = 0.49$).

Inter- and Intraobserver Variability (2D-FT MRI)

The intraobserver CoV for GLS was 11.5% and for GLSR 8.9%. The interobserver CoV for GLS was 10.7% and for GLSR 18.2%.

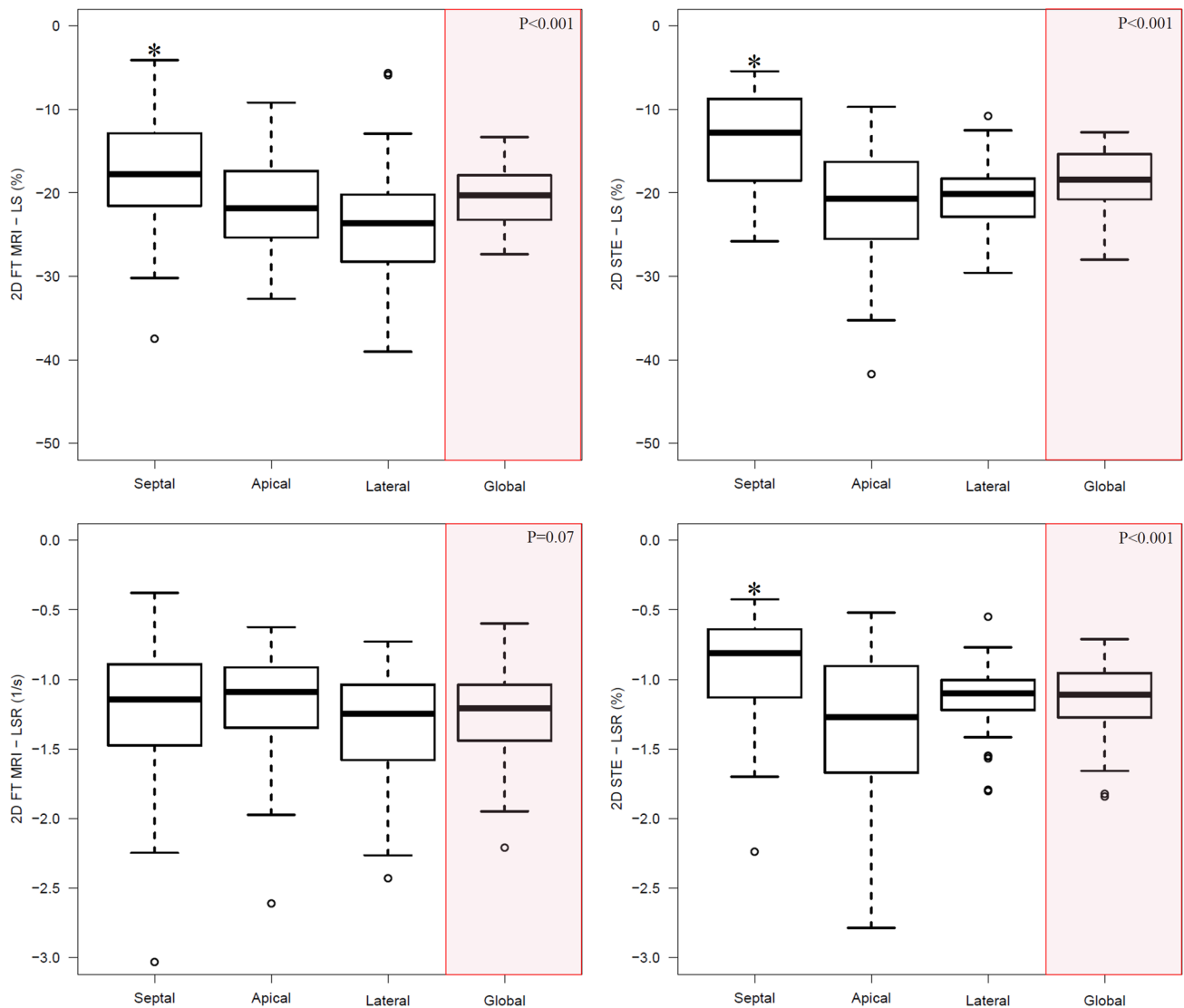


Fig. 4 Comparison between regional and global LS and LSR derived by 2D-FT MRI (left) und 2D-STE (right). *p* values refer to overall group comparison and the star symbol (*) indicates significant difference between septal segment and other two segments in post hoc analysis

Table 3 Intraventricular dyssynchrony using 2D-FT MRI and 2D-STE

	Septal T2PLS (ms)	Lateral T2PLS (ms)	Wall-to-wall delay (ms)
2D-FT MRI	305.5 [36.5, 687.0]	332.5 [175.5, 493.0]	-27.5 [-235.0, 384.0]
2D-STE	370.5 [246.0, 493.0]	364.5 [258.0, 453.0]	24.5 [-123.0, 116.0]
<i>p</i> value	0.002	0.012	0.10

Data are expressed as median, minimum, and maximum values

T2PLS time to peak longitudinal strain. *p* values refer to Mann–Whitney *U* test

Discussion

In our cohort of HLHS patients, regional and global myocardial longitudinal deformation parameters could easily be assessed with new 2D-FT-MRI technique. Visualization

was excellent in all myocardial segments and allowed measurements of LS and LSR in all patients included in this study. For septal and lateral segments, we found an acceptable agreement with LS measured by 2D-STE.

Measuring myocardial deformation parameters with MRI is not entirely new. In the past different techniques, such as

CMR tagging [14], strain-encoding (SENC) [15], or displacement encoding with stimulated echoes (DENSE), MRI [16] have been used. The advantage of the new 2D-FT-MRI technique is clearly that it is a post-processing software which can be performed on any routine gradient echo MR images. Therefore, no extra scanning time is needed, which is especially valuable when scanning young and, therefore, sedated children.

Previous Studies Using 2D-FT MRI to Analyze Ventricular Function in Congenital Heart Disease

Some studies already investigated ventricular function of patients with congenital heart diseases using 2D-FT MRI [10, 17–19]. Similar to our results, they reported excellent feasibility of the method. Schmidt et al. used 2D-FT-MRI for the first time in Fontan patients [11]. They analyzed longitudinal and circumferential strain and strain rate in a cohort of 15 adult Fontan patients with heterogeneous ventricular anatomy and concluded that 2D-FT-MRI could have clinical relevance in this patient cohort in the future since FT results seem to relate to symptoms and objective exercise tolerance. In contrast to our study, only one patient with a single RV was included. Recently Ghelani et al. analyzed ventricular deformation in 134 Fontan patients including 60 patients with a dominant RV using 2D FT-MRI and reported good reproducibility of this technique in the single RV [10]. For the subpulmonary RV normal deformation, data have been published for adults and pooled in a meta analysis of nine 2D-FT MRI studies [20]. Unfortunately, reference values of 2D-FT MRI myocardial deformation parameters for children with a structurally normal heart are still lacking. A systematic problem is the comparison of single RV deformation data with data of a subpulmonary RV in the biventricular heart. This comparison has been done with 2D STE technique, where Moiduddin et al. [21] showed lower deformation of the systemic RV in Fontan patients compared to the subpulmonary RV of age-matched controls.

In the past decade, 2D-STE has been established as a technique to quantify systolic and diastolic ventricular function in congenital heart disease. Various studies have shown that it can be correctly applied in HLHS patients throughout all stages of Fontan palliation [4, 7, 21]. Moreover, a simultaneous study using 2D-STE and conductance catheters in HLHS Fontan patients from our center has shown that RV LSR correlated well with systolic elastance, a parameter of contractility [5]. We, therefore, compared our 2D-FT MRI results with 2D-STE. Since we find it difficult to standardize echocardiographic short axis views of the systemic RV, we only assessed longitudinal deformation in the four chamber view. For GLS and GLSR, results of our cohort are comparable with previously published values of HLHS patients [4, 21, 22].

Comparison of 2D-FT MRI and 2D-STE Deformation Parameters

For GLS, we found a clinically acceptable agreement between the MRI and STE. 2D-FT MRI slightly underestimates LS values. Schmidt et al. and Ghelani et al. used the same two imaging modalities to compare longitudinal deformation in Fontan patients [10, 11]. Schmidt et al. report only a modest agreement between 2D-FT MRI and 2D-STE in the single LV which they explain by poor reproducibility of 2D-STE due to bad visualization of myocardial segments with poor acoustic windows particularly in older patients. The patients in their study cohort were adults with a mean age of 27.4 years. For pediatric HLHS, patients-acceptable intraobserver agreement for 2D-STE LS and LSR has repeatedly been published [4, 7]. Therefore, the slightly better agreement of the two modalities might be related to better reproducibility of STE parameters in our patient cohort. In line with our findings, Ghelani et al. found better agreement for GLS in the systemic RV than the LV of Fontan patients with a median age of 16.8 years [10]. The agreement in the regional LS was not as good especially in the apical segments. The apical segment is often difficult to visualize entirely in echocardiography and almost one-third of the apical segments could not be evaluated in the present study. In contrast to our study, Singh et al. showed a high correlation between CMR- and STE-derived strain measures in Fontan patients with a single LV. However, they used CMR tagging to measure strain and since patients were recruited prospectively, standard frame rates could be used in STE which might account for the higher degree of correlation [23].

The wide limits of agreement in Bland-Altman plot show that for GLSR, the agreement between 2D-FT MRI and 2D-STE was poor. Since strain rate is the time-derivative of strain, the difference in temporal resolution between the two imaging modalities might account for the poor agreement [24]. Temporal resolution in MRI can be a problem with higher heart rates in small children. In our study, median frame rate of STE was 85/s, which should be sufficient for the median heart rate of 81 bpm. In MRI, however, median number of heart phases was 25 [20–30]. We presume that in order to detect changes in strain rate, a higher temporal resolution than 28.8 ms is required [13]. For the LV of healthy volunteers, Orwat et al. reported a poor agreement of longitudinal and circumferential GSR between 2D-FT MRI and 2D-STE [25]. They also attributed the poor agreement to the difference in temporal resolution between the methods.

Regional LS and LSR in all HLHS Patients

Looking at the three segments of the RV in all patients, the regional LS was significantly reduced in the septal segments compared to the apical and lateral segments in 2D-FT MRI

as well as in 2D-STE. This pattern has been shown before and attributed to the adjacent remnant of the left ventricle to the septal segment in HLHS patients. For regional LSR, 2D-FT MRI showed no differences in the segments, while 2D-STE showed the same pattern as with LS, with lower LSR in the septal segment.

Relation Between the Myocardial Deformation Parameters and Demographic and Clinical Data

For clinical routine, EF is the only established parameter to assess RV function. MRI has been the gold standard for measuring EF for many years. In our study, we show a good correlation of GLS and moderate correlation of GLSR with RV EF derived by 2D-FT MRI. Up to date, correlation of 2D-STE deformation parameters with RV EF derived by MRI has been shown. In the systemic RV of patients after atrial switch operation, Chow et al. found a good correlation of 2D-STE-derived GLSR with EF but not with GLS [26]. On the other hand, Smith et al. found a good correlation between 3D echocardiographic RV EF and LS in patients with pulmonary hypertension, where the RV is also subjected to chronic pressure load [27]. In addition, for the volume-loaded RV of TOF patients, a good agreement of RV EF and STE-derived GLS was shown [28]. The better correlation of GLS with EF in our study is feasible since 2D-STE-derived GLSR has been shown to be a load independent index of contractility in HLHS patients, whereas GLS and EF are load-dependent [5].

In our study, GLS and GLSR did not correlate with age, BSA, HR, SO_2 , and gender. This finding is in agreement with a meta analysis by Levy et al. who found the variation in GLS and GLSR in ten different echocardiographic studies of healthy children did not depend on the differences in age, gender, BSA, and HR [29]. Moreover, Lorch et al. didn't find any significant age-related changes for GLS in the LV of healthy children, whereas GLSR declined in the first 10 years after birth [30].

Intraventricular Systolic Dyssynchrony

Quantification of RV dyssynchrony can be useful to identify uncoordinated contraction [22, 31]. The T2PLS in the lateral and septal segment was significantly different between 2D-FT MRI and 2D-STE. This is not surprising as the two imaging modalities use different segmentation. Moreover, the T2PLS in 2D-STE is calculated from the beginning of the QRS whereas in MRI datasets, a simultaneous electrocardiogram signal is not available in the post-processing software and the beginning of the systole is automatically set. However, calculated wall-to-wall delay was not different between both methods, even if the median was negative in MRI and positive in STE; for the single RV positive as well

as negative values have been published using STE [22, 32]. It has been shown that a larger rudimentary LV causes a delay in septal motion and thus causes greater dyssynchrony and that single RVs have increased dyssynchrony compared to healthy controls [33]. Although some studies suspect that higher RV dyssynchrony might influence RV function in the single ventricle, the impact of dyssynchrony in HLHS patients has yet to be proven by longer follow-up studies. From a technical point of view, measuring dyssynchrony with 2D-STE is more accurate than with 2D-FT-MRI.

Study Limitations

The 2D-FT MRI software, such as 2D-STE, was designed for the analysis of myocardial deformation parameters in normal subjects [9, 34]. Therefore, allocation and terminology of the seven segments does not always correlate with the anatomical structure of the heart in HLHS patients, particularly in absence of the LV.

The segmentation of the myocardium in six or seven segments is automatically performed by the software and cannot be influenced by the user. We, therefore, had to adapt the segmentation to be able to compare the two imaging modalities which might reduce the accuracy of our results for the regional parameters.

Patients in BCPC and TCPC were included in the study. Because patients were not investigated longitudinally, and fewer patients were in BCPC stage, we did not focus on comparing the two cohorts. However, to ascertain that all patients can be regarded as a single group, we tested for differences between the stages. In our opinion, the only minor differences found in GLSR can be neglected and we, therefore, joint both patient groups for further analysis.

Finally, the intraobserver variability of 2D-FT MRI parameters of about 8.9–10.5% and interobserver variability of about 10.7–18.2% have to be considered when interpreting the results.

Conclusions

CMR images allow excellent visualization of the myocardium of the single RV in HLHS patients. Measuring myocardial deformation with 2D-FT MRI is feasible in these particular patients and can be easily performed with post-processing software without the necessity of extra scanning time. Agreement with 2D-STE is acceptable for LS but poor for LSR. The lower temporal resolution of MRI might account for the poor agreement between the imaging modalities. Future longitudinal studies are warranted to evaluate whether 2D-FT MRI deformation parameters can be used for early detection of heart failure in this special patient population.

Acknowledgements The authors thank Mrs. Traudel Hansen and Mrs. Gabriele Kroeger for their assistance in patient management, Dr. Marka-Jill Jussli-Melchers and Dr. Jens Groebner for clinical and technical comments.

Compliance with Ethical Standards

Conflict of interest The authors declare that they have no conflict of interest.

Ethical Approval The study was performed according to the protocol (No. AZ 168/07) approved by the institutional ethics committee and in accordance with the ethical standards laid down in the 1964 declaration of Helsinki and its later amendments.

Informed Consent All parents or legal guardians gave their informed consent in a written form.

References

- Altmann K, Printz BF, Solowiejczyk DE, Gersony WM, Quaegebeur J, Apfel HD (2000) Two-dimensional echocardiographic assessment of right ventricular function as a predictor of outcome in hypoplastic left heart syndrome. *Am J Cardiol* 86:964–968
- Bell A, Bellsham-Revell HR, Beerbaum P, Razavi R, Greil G (2011) Inter-stage right ventricular remodeling in hypoplastic left heart syndrome. *J Cardiovasc Magn Reson* 13:P205
- Feinstein JA, Benson DW, Dubin AM, Cohen MS, Maxey DM, Mahle WT et al (2012) Hypoplastic left heart syndrome: current considerations and expectations. *J Am Coll Cardiol* 59:42
- Petko C, Uebing A, Furck A, Rickers C, Scheewe J, Kramer H-H (2011) Changes of right ventricular function and longitudinal deformation in children with hypoplastic left heart syndrome before and after the Norwood operation. *J Am Soc Echocardiogr* 24:1226–1232
- Schlangen J, Petko C, Hansen JH, Michel M, Hart C, Uebing A et al (2014) Two-dimensional global longitudinal strain rate is a preload independent index of systemic right ventricular contractility in hypoplastic left heart syndrome patients after Fontan operation. *Circ Cardiovasc Imaging* 7:880–886
- Khoo NS, Smallhorn JF, Kaneko S, Myers K, Kutty S, Tham EB (2011) Novel insights into RV adaptation and function in hypoplastic left heart syndrome between the first 2 stages of surgical palliation. *JACC Cardiovasc Imaging* 4:128–137
- Michel M, Logoteta J, Entenmann A, Hansen JH, Voges I, Kramer H-H, Petko C (2016) Decline of systolic and diastolic 2D strain rate during follow-up of HLHS patients after Fontan palliation. *Pediatr Cardiol* 37:1250–1257
- Voigt J-U, Pedrizzetti G, Lysyansky P, Marwick TH, Houle H, Baumann R et al (2015) Definitions for a common standard for 2D speckle tracking echocardiography: consensus document of the EACVI/ASE/industry task force to standardize deformation imaging. *J Am Soc Echocardiogr* 28:183–193
- Hor KN, Gottliebson WM, Carson C, Wash E, Cnota J, Fleck R et al (2010) Comparison of magnetic resonance feature tracking for strain calculation with harmonic phase imaging analysis. *JACC Cardiovasc Imaging* 3:144–151
- Ghelani SJ, Harrild DM, Gauvreau K, Geva T, Rathod RH (2016) Echocardiography and magnetic resonance imaging based strain analysis of functional single ventricles: a study of intra- and inter-modality reproducibility. *Int J Cardiovasc Imaging* 32:1113–1120
- Schmidt R, Orwat S, Kempny A, Schuler P, Radke R, Kahr PC et al (2014) Value of speckle-tracking echocardiography and MRI-based feature tracking analysis in adult patients after Fontan-type palliation. *Congenit Heart Dis* 9:397–406
- Pruessmann KP, Weiger M, Scheidegger MB, Boesiger P (1999) SENSE: sensitivity encoding for fast MRI. *Magn Reson Med* 42:952–962
- Claus P, Omar AMS, Pedrizzetti G, Sengupta PP, Nagel E (2015) Tissue tracking technology for assessing cardiac mechanics: principles, normal values, and clinical applications. *JACC Cardiovasc Imaging* 8:1444–1460
- Oxenham HC, Young AA, Cowan BR, Gentles TL, Occleshaw CJ, Fonseca CG et al (2003) Age-related changes in myocardial relaxation using three-dimensional tagged magnetic resonance imaging. *J Cardiovasc Magn Reson* 5:421–430
- Neizel M, Lossnitzer D, Korosoglou G, Schaufele T, Lewien A, Steen H et al (2009) Strain-encoded (SENC) magnetic resonance imaging to evaluate regional heterogeneity of myocardial strain in healthy volunteers: comparison with conventional tagging. *J Magn Reson Imaging* 29:99–105
- Mangion K, Clerfond G, McComb C, Carrick D, Rauhalammi SM, McClure J et al (2016) Myocardial strain in healthy adults across a broad age range as revealed by cardiac magnetic resonance imaging at 1.5 and 3.0T: associations of myocardial strain with myocardial region, age, and sex. *J Magn Reson Imaging* 44:1197–1205
- Kempny A, Fernandez-Jimenez R, Orwat S, Schuler P, Bunck AC, Maintz D et al (2012) Quantification of biventricular myocardial function using cardiac magnetic resonance feature tracking, endocardial border delineation and echocardiographic speckle tracking in patients with repaired tetralogy of Fallot and healthy controls. *J Cardiovasc Magn Reson* 14:32
- Anwar S, Harris MA, Whitehead KK, Keller MS, Goldmuntz E, Fogel MA, Mercer-Rosa L (2017) The impact of the right ventricular outflow tract patch on right ventricular strain in tetralogy of fallot: a comparison with valvar pulmonary stenosis utilizing cardiac magnetic resonance. *Pediatr Cardiol* 38:617–623
- Heiberg J, Ringgaard S, Schmidt MR, Redington A, Hjortdal VE (2015) Structural and functional alterations of the right ventricle are common in adults operated for ventricular septal defect as toddlers. *Eur Heart J Cardiovasc Imaging* 16:483–489
- Vo HQ, Marwick TH, Negishi K (2017) MRI-derived myocardial strain measures in normal subjects. *JACC Cardiovasc Imaging* 11:196–205
- Tham EB, Smallhorn JF, Kaneko S, Valiani S, Myers KA, Colen TM et al (2014) Insights into the evolution of myocardial dysfunction in the functionally single right ventricle between staged palliations using speckle-tracking echocardiography. *J Am Soc Echocardiogr* 27:314–322
- Moiduddin N, Texter KM, Zaidi AN, Hershenson JA, Stefaniak CA, Hayes J, Cua CL (2010) Two-dimensional speckle strain and dyssynchrony in single right ventricles versus normal right ventricles. *J Am Soc Echocardiogr* 23:673–679
- Singh GK, Cupps B, Pasque M, Woodard PK, Holland MR, Ludomirsky A (2010) Accuracy and reproducibility of strain by speckle tracking in pediatric subjects with normal heart and single ventricular physiology: a two-dimensional speckle-tracking echocardiography and magnetic resonance imaging correlative study. *J Am Soc Echocardiogr* 23:1143–1152
- Pedrizzetti G, Claus P, Kilner PJ, Nagel E (2016) Principles of cardiovascular magnetic resonance feature tracking and echocardiographic speckle tracking for informed clinical use. *J Cardiovasc Magn Reson* 18:51
- Orwat S, Kempny A, Diller G-P, Bauerschmitz P, Bunck AC, Maintz D et al (2014) Cardiac magnetic resonance feature tracking: a novel method to assess myocardial strain. Comparison with

- echocardiographic speckle tracking in healthy volunteers and in patients with left ventricular hypertrophy. *Kardiol Pol* 72:363–371
26. Chow P-C, Liang X-C, Cheung EWY, Lam WWM, Cheung Y-F (2008) New two-dimensional global longitudinal strain and strain rate imaging for assessment of systemic right ventricular function. *Heart* 94:855–859
 27. Smith BCF, Dobson G, Dawson D, Charalampopoulos A, Grapsa J, Nihoyannopoulos P (2014) Three-dimensional speckle tracking of the right ventricle: toward optimal quantification of right ventricular dysfunction in pulmonary hypertension. *J Am Coll Cardiol* 64:41–51
 28. Almeida-Morais L, Pereira-da-Silva T, Branco L, Timoteo AT, Agapito A, de Sousa L et al. (2016) The value of right ventricular longitudinal strain in the evaluation of adult patients with repaired tetralogy of Fallot: a new tool for a contemporary challenge. *Cardiol Young* 2016:1–9
 29. Levy PT, Sanchez Mejia AA, Machefsky A, Fowler S, Holland MR, Singh GK (2014) Normal ranges of right ventricular systolic and diastolic strain measures in children: a systematic review and meta-analysis. *J Am Soc Echocardiogr* 27:549
 30. Lorch SM, Ludomirsky A, Singh GK (2008) Maturation and growth-related changes in left ventricular longitudinal strain and strain rate measured by two-dimensional speckle tracking echocardiography in healthy pediatric population. *J Am Soc Echocardiogr* 21:1207–1215
 31. Lopez-Candales A, Dohi K, Bazaz R, Edelman K (2005) Relation of right ventricular free wall mechanical delay to right ventricular dysfunction as determined by tissue Doppler imaging. *Am J Cardiol* 96:602–606
 32. Petko C, Hansen JH, Scheewe J, Rickers C, Kramer H-H (2012) Comparison of longitudinal myocardial deformation and dyssynchrony in children with left and right ventricular morphology after the Fontan operation using two-dimensional speckle tracking. *Congenit Heart Dis* 7:16–23
 33. Petko C, Voges I, Schlangen J, Scheewe J, Kramer H-H, Uebing AS (2011) Comparison of right ventricular deformation and dyssynchrony in patients with different subtypes of hypoplastic left heart syndrome after Fontan surgery using two-dimensional speckle tracking. *Cardiol Young* 21:677–683
 34. Maret E, Todt T, Brudin L, Nylander E, Swahn E, Ohlsson JL, Engvall JE (2009) Functional measurements based on feature tracking of cine magnetic resonance images identify left ventricular segments with myocardial scar. *Cardiovasc Ultrasound* 7:53